Slow diffusive structure in Nikolaevskii turbulence

Takayuki Narumi [1,*] and Yoshiki Hidaka [2]

[1] *Graduate School of Sciences and Technology for Innovation, Yamaguchi University, Ube 755-8611, Japan*
[2] *Faculty of Engineering, Kyushu University, Fukuoka 819-0395, Japan*

(Received 2 October 2019; revised manuscript received 19 December 2019; accepted 16 January 2020; published 3 February 2020)

Weak turbulence has been investigated in nonlinear-nonequilibrium physics to understand universal characteristics near the transition point of ordered and disordered states. Here the one-dimensional Nikolaevskii turbulence, which is a mathematical model of weak turbulence, is studied theoretically. We calculate the velocity field of the Nikolaevskii turbulence assuming a convective structure and carry out tagged-particle simulations in the flow to clarify the Nikolaevskii turbulence from the Lagrangian description. The tagged particle diffuses in the disturbed flow and the diffusion is superdiffusive in an intermediate timescale between ballistic and normal-diffusive scale. The diffusion of the slow structure is characterized by the power law for the control parameter near the transition point of the Nikolaevskii turbulence, suggesting that the diffusive characteristics of the slow structure remain scale invariant. We propose a simplified model, named two-scale Brownian motion, which reveals a hierarchy in the Nikolaevskii turbulence.

DOI: 10.1103/PhysRevE.101.022202

I. INTRODUCTION

Turbulence appears in all areas of nature, from microscopic to macroscopic levels. Most studies of turbulence have targeted fully developed turbulence, which is regarded as a flow regime characterized by a strong velocity disturbance in the spatiotemporal region. Highly enhanced transport properties are measured as turbulent diffusion or chaotic advection [1,2]. On the other hand, since the pioneering work by Reynolds [3], research into what happens at the beginning of disturbance is still active [4–6]. Weak turbulence introduced by Manneville [7] derived from the study to understand the transition between ordered and disordered states. The pattern in weak turbulence is disordered as a whole but maintains local order. For example, the local order is convection rolls in the turbulent transition of convective systems; in fact, weak turbulence is experimentally obtained in nematic electroconvective systems [8,9]. Weak turbulence is modeled by deterministic chaos for confined systems or spatiotemporal chaos for extended systems. In this paper we study a type of spatiotemporal chaos, Nikolaevskii turbulence, from the Lagrangian description and aim to understand the transport characteristics of weak turbulence in a statistical-physics manner.

Nikolaevskii turbulence is defined as a spatially and temporally chaotic solution of the Nikolaevskii equation

$$\frac{\partial \phi(\boldsymbol{x},t)}{\partial t} + [\nabla \phi(\boldsymbol{x},t)]^2 = -\nabla^2[\varepsilon - (1+\nabla^2)^2]\phi(\boldsymbol{x},t), \quad (1)$$

with the control parameter ε. The one-dimensional case is equivalent to the model for longitudinal seismic waves proposed by Nikolaevskii [10]. Tribelsky and Tsuboi showed that the solutions bifurcate supercritically from a spatially uniform state to a turbulent regime, i.e., Nikolaevskii turbulence [11]. The Nikolaevskii equation is a pattern-forming system with the Galilean symmetry $\boldsymbol{x} \to \boldsymbol{x} + \boldsymbol{U}t$, $\nabla\phi \to \nabla\phi + \boldsymbol{U}$ [12], or with the symmetry under the transformation $\phi \to \phi +$ const [11]. This symmetry indicates the infinite relaxation time for the overall translational movement of ϕ. It leads to a long-wavelength neutral mode, i.e., Nambu-Goldstone mode [13,14], which interacts with short-wavelength modes to make spatially periodic steady solutions unstable. From the viewpoint of phase dynamics, Eq. (1) is derived as a phase equation of an oscillatory reaction-diffusion system [15–17]. In experiments, a kind of weak turbulence seen in nematic electroconvective systems, called soft-mode turbulence [18–20], is considered to correspond to the Nikolaevskii turbulence.

Tanaka proved that Nikolaevskii turbulence is equivalent to a type of spatiotemporal chaos exhibited in a complex Ginzburg-Landau equation with nonlocal coupling [16]. This implies that a nonlocal structure can emerge in disorder flow in Nikolaevskii turbulence. Indeed, the Matthews-Cox equations, which are the amplitude equations derived from the Nikolaevskii equation, show a global structure characterized by the coexistence of disorder and an amplitude death state [21]. Sakaguchi and Tanaka investigated such a structure in Nikolaevskii turbulence [21], while the properties have been left unclear.

Studies for fluid dynamics are divided roughly into Eulerian or Lagrangian description. Tanaka and Okamura investigated the modal and total time correlation functions for $\partial\phi/\partial x$ of the Nikolaevskii equation [22]. Their study is based on the Eulerian description. However, it is inconvenient to study transport phenomena; instead, it is more convenient to use the Lagrangian description. We study the one-dimensional Nikolaevskii equation through numerical simulation of tagged particles and focus on diffusive properties of the tagged particles. The diffusion in fully developed turbulence is normal at

*tnarumi@yamaguchi-u.ac.jp;
http://web.cc.yamaguchi-u.ac.jp/~tnarumi/

any macroscopic timescales [23], while in weak turbulence it is expected to be not normal because of local order. Thus, the study of anomalous diffusion will lead to an understanding of the characteristics of weak turbulence.

The present paper is organized as follows. Section II explains the Nikolaevskii turbulence and the numerical simulation of tagged-particle dynamics. Section III shows the results of the particle dynamics. To understand the results, a schematic model is investigated analytically in Sec. IV. Section V summarizes this paper.

II. MODEL AND NUMERICAL CALCULATION

We study the one-dimensional Nikolaevskii equation for $\phi = \phi(x,t)$,

$$\frac{\partial \phi}{\partial t} + \left(\frac{\partial \phi}{\partial x}\right)^2 = -\frac{\partial^2}{\partial x^2}\left[\varepsilon - \left(1 + \frac{\partial^2}{\partial x^2}\right)^2\right]\phi. \quad (2)$$

The dispersion relation of Eq. (2) is

$$\lambda = k^2[\varepsilon - (1 - k^2)^2]. \quad (3)$$

In addition to the Nambu-Goldstone mode at $k = 0$, the unstable mode around $k = 1$ appears for $\varepsilon > 0$. Since it interacts with the long-wavelength mode, any steady periodic solutions do not appear; instead, the chaotic solutions emerge supercritically at $\varepsilon = 0$ [11].

We numerically solved Eq. (2) under a periodic boundary condition with the system length $L = 2^{12}$ and the space increment $\Delta x = 2^{-1}$. Although the behavior is affected by the value of L especially at small ε, it was confirmed that L is independent of the results of the ε range shown in this paper [24]. The equation was solved by a pseudospectral method and the time stepping was done by the exponential time differencing scheme of the second-order Runge-Kutta methods [25] with the time increment $\Delta t = 10^{-2}$. The zero mode was not taken into account in numerical calculations as we did not consider the translational motion of the whole system [11]. The initial condition of ϕ was the perturbation around $\phi = 0$ and the system waits to reach a steady state before sampling, with a waiting time of $t_w = 10^5$.

The convective system is a nonlinear-nonequilibrium system with a periodic structure. Herein we regard the modes around $k = 1$ of the Nikolaevskii equation as convective modes. This makes it possible to compare our theoretical results with the experimental results of the convection systems. In fact, soft-mode turbulence, which is a weak turbulence corresponding to Nikolaevskii turbulence, is found in a nematic electroconvective system. We then expand the system in the z direction in the range $0 \leqslant z \leqslant \pi$, so symmetric convective rolls can exist on the x-z plane. If we suppose that ϕ is the phase, the velocity in the x direction should be proportional to $\partial\phi/\partial x$, which is the local wave number [26]. Thus, to obtain the convective velocity field $\boldsymbol{v} = \boldsymbol{v}(x, z, t)$ from $\phi = \phi(x,t)$, we employ

$$\boldsymbol{v} = (v_x, v_z) = \left(-\frac{\partial \phi}{\partial x}\frac{dF}{dz}, \frac{\partial^2 \phi}{\partial x^2}F\right), \quad (4)$$

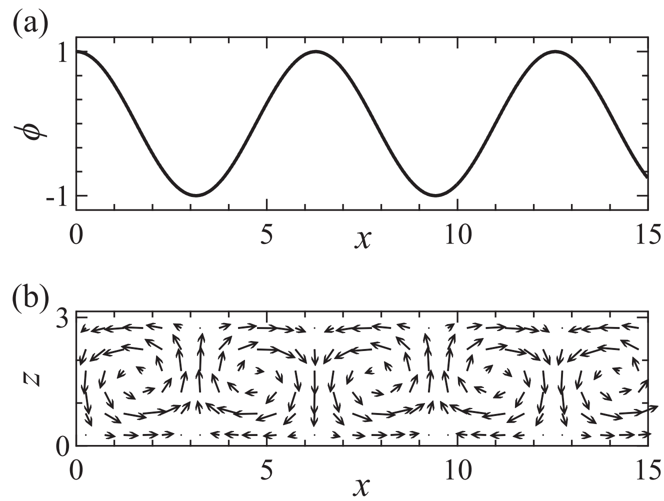

FIG. 1. Profile of (a) ϕ and (b) the corresponding velocity field in the case $\phi = \cos x$.

where

$$F(z) = \left(\frac{2z}{\pi}\right)^2\left(2 - \frac{2z}{\pi}\right)^2 \quad (5)$$

is a function characterizing convection with the rigid boundary condition in the z direction [27]. The velocity field satisfies the condition of incompressibility: $\nabla \cdot \boldsymbol{v} = 0$. Figure 1 shows the velocity field on the x-z plane in the case $\phi(x,t) = \cos x$ as an example.

Under the condition that the mass of the tagged particle is small and/or the friction coefficient is large, the tagged-particle velocity $\boldsymbol{V}(t) = (V_x(t), V_z(t))$ is equivalent to the velocity field, that is,

$$\boldsymbol{V}(t) = (v_x(X(t), Z(t), t), v_z(X(t), Z(t), t)), \quad (6)$$

where $\boldsymbol{X}(t) = (X(t), Z(t))$ denotes the tagged-particle position. As the velocity field $\boldsymbol{v}$ is obtained discretely, the tagged-particle velocity $\boldsymbol{V}(t)$ is calculated as

$$\boldsymbol{V}(t) = (1 - p)\boldsymbol{v}(x^*, Z(t), t) + p\boldsymbol{v}(x^* + \Delta x, Z(t), t), \quad (7)$$

where x^* is a grid point satisfying $x^* \leqslant X(t) \leqslant x^* + \Delta x$ and $p = [X(t) - x^*]/\Delta x$. One can obtain the tagged-particle dynamics from the solutions of the Nikolaevskii turbulence through the evolution equation

$$\boldsymbol{X}(t + \Delta t) = \boldsymbol{X}(t) + \boldsymbol{V}(t)\Delta t. \quad (8)$$

An example of how a tagged particle moves on the x axis is shown in Fig. 2.

The tagged particle is set as a rigid circle to keep the particle from sticking to the boundary. The radius is $a = 0.2$, which was set up corresponding to the experimental conditions [28]. Note that the value has little effect on the following simulation results. The boundary condition of the tagged-particle dynamics is periodic in the x direction and rigid in the z direction, that is, the tagged particle undergoes elastic collision with the boundary in the z direction.

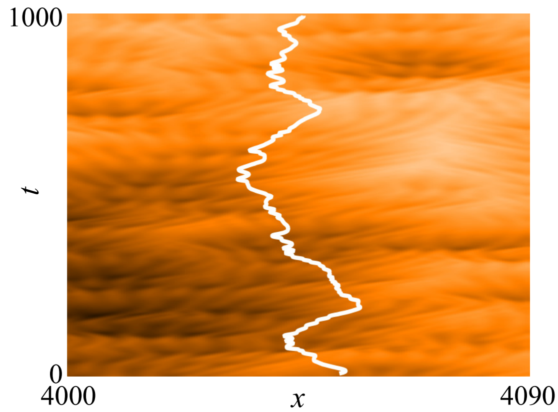

FIG. 2. Spatiotemporal pattern and tagged-particle trajectory at $\varepsilon = 0.1$. The color indicates the value of $\phi(x,t)$. The white line represents the trajectory of a tagged particle.

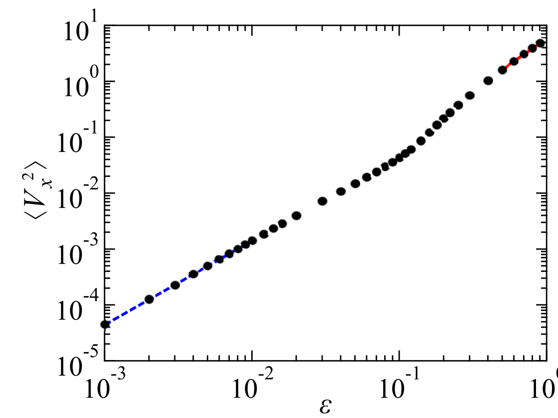

FIG. 4. The ε dependence of the mean-square velocity of the ballistic motion in the shortest timescale. The blue dashed line and red solid line represent the power-law fitting (10).

III. RESULTS

A. Mean-square displacement

Turbulent flow diffuses tagged particles. The diffusive property can be characterized by the mean-square displacement. We take account of movement only in the x direction,

$$M_2(\tau) = \langle |X(t+\tau) - X(t)|^2 \rangle, \tag{9}$$

where the angular brackets denote the sample average in the steady state. Figure 3 shows the simulation results of the mean-square displacement, each of which is obtained by averaging 10^7 time-series data. The computation in this work has been done using the supercomputer system ITO, Kyushu University. The dynamics is ballistic in the shortest timescale. We consider an effective temperature, which is proportional to the mean-square velocity $\langle V_x^2 \rangle$, as an indicator of the randomness that tagged particles receive. Figure 4 indicates that T is well described by the power law as

$$T \sim \begin{cases} \varepsilon^{\alpha_\mathrm{l}} & (\text{low } \varepsilon) \\ \varepsilon^{\alpha_\mathrm{h}} & (\text{high } \varepsilon), \end{cases} \tag{10}$$

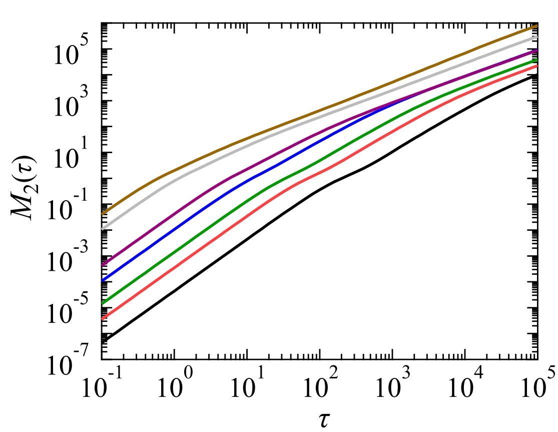

FIG. 3. The x-direction mean-square displacement calculated from tagged-particle dynamics. The solid lines represent the numerical results of $\varepsilon = 0.001$ (black), 0.004 (red), 0.01 (green), 0.04 (blue), 0.1 (purple), 0.4 (gray), and 0.8 (brown), from bottom to top.

with $\alpha_\mathrm{l} = 1.50 \pm 0.00$ and $\alpha_\mathrm{h} = 1.86 \pm 0.02$. As Tanaka has stated, from the viewpoint of the energy spectrum, solutions of the Nikolaevskii equation at $\varepsilon > 0.1$ are qualitatively indistinguishable from those for Kuramoto-Sivashinsky turbulence [29]. Nugroho *et al.* also show the crossover behavior around $\varepsilon \simeq 0.1$ [30]. Thus, the power α_l is a feature of the Nikolaevskii turbulence and the power α_h is that of the Kuramoto-Sivashinsky-type turbulence.

Matthews and Cox explained theoretically a self-consistent scaling as $\partial\phi/\partial x \sim \varepsilon^{3/4} A(X,T)\exp(ix) + \text{c.c.} + \varepsilon f(X,T)$, with $T = \varepsilon t$ and $X = \varepsilon^{1/2} x$. The square of the leading term is of order $\varepsilon^{3/2}$, which agrees with α_l.

Hidaka *et al.* measured the effective temperature of the soft-mode turbulence and revealed that the temperature is proportional to the control parameter $\varepsilon_\mathrm{expt}$ in the experiment [31]. Our simulation result thus implies the relationship of the control parameters between the soft-mode turbulence and the Nikolaevskii turbulence as $\varepsilon_\mathrm{expt} \sim \varepsilon^{2/3}$, but more detailed consideration is needed.

B. Diffusion coefficient

To study the dynamics except for the shortest, i.e., ballistic, timescale, we calculate the time-dependent diffusion coefficient

$$D(\tau) = \frac{M_2(\tau)}{2\tau}. \tag{11}$$

We confirm that every $D(\tau)$ at $\varepsilon \geqslant 0.003$ converges at the longest timescale. This means that the tagged particle normally diffuses at the longest timescale. On the other hand, for $\varepsilon < 0.003$, $D(\tau)$ gently increases with time within our observation time $\tau \leqslant 10^5$. We believe that chaotic characteristics impose that the diffusion type for extremely low ε also becomes normal, that is $D(\tau)$ becomes a constant, at a sufficiently long time.

The convergence value of $D(\tau)$ is the long-time diffusion coefficient $D_\mathrm{LT} = \lim_{\tau\to\infty} D(\tau)$. Figure 5 indicates that D_LT is described by the power law as

$$D_\mathrm{LT} \sim \begin{cases} \varepsilon^{\beta_\mathrm{l}} & (\text{low } \varepsilon) \\ \varepsilon^{\beta_\mathrm{h}} & (\text{high } \varepsilon), \end{cases} \tag{12}$$

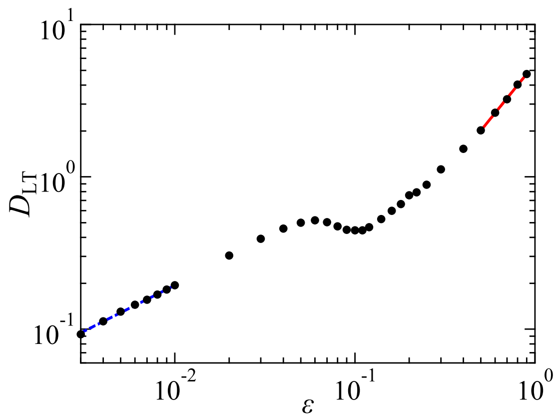

FIG. 5. The ε dependence of the long-time self-diffusion coefficient. The blue dashed line and the red solid line represent the power-law fitting (12).

with $\beta_l = 0.597 \pm 0.011$ and $\beta_h = 1.46 \pm 0.03$. We will discuss the value of β_l in Sec. IV C.

C. Anomalous parameter

Diffusion can become anomalous in complex systems, which is collectively called anomalous diffusion [32]. The anomalous diffusion is characterized by the anomalous parameter γ, defined in $D(\tau) \propto \tau^{\gamma}$. We investigate the timescale dependence of γ calculated as

$$\gamma(\tau) = \frac{d \ln D(\tau)}{d \ln \tau}. \tag{13}$$

As shown in Fig. 6, the anomalous parameter decreases until the time reaches the local minimum, increases until the time reaches the local maximum, and then decreases gently to converge to zero. The anomalous parameter for the conventional Brownian motion monotonically decreases from $\lim_{\tau\to 0} \gamma(\tau) = 1$ to $\lim_{\tau\to\infty} \gamma(\tau) = 0$. We can thus conclude that the tagged particle in the Nikolaevskii turbulence anomalously diffuses in the intermediate timescale. The

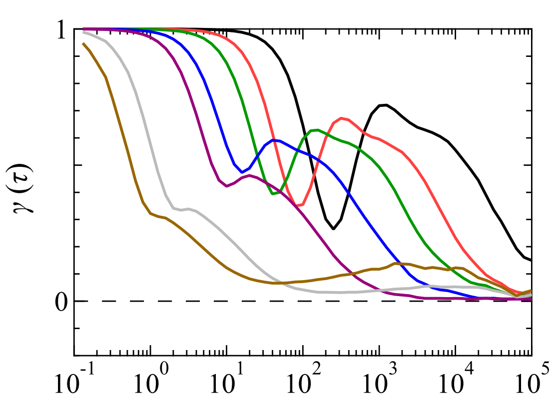

FIG. 6. Anomalous parameter calculated from tagged-particle dynamics. The solid lines represent the numerical results of $\varepsilon = 0.001$ (black), 0.004 (red), 0.01 (green), 0.04 (blue), 0.1 (purple), 0.4 (gray), and 0.8 (brown), from right to left.

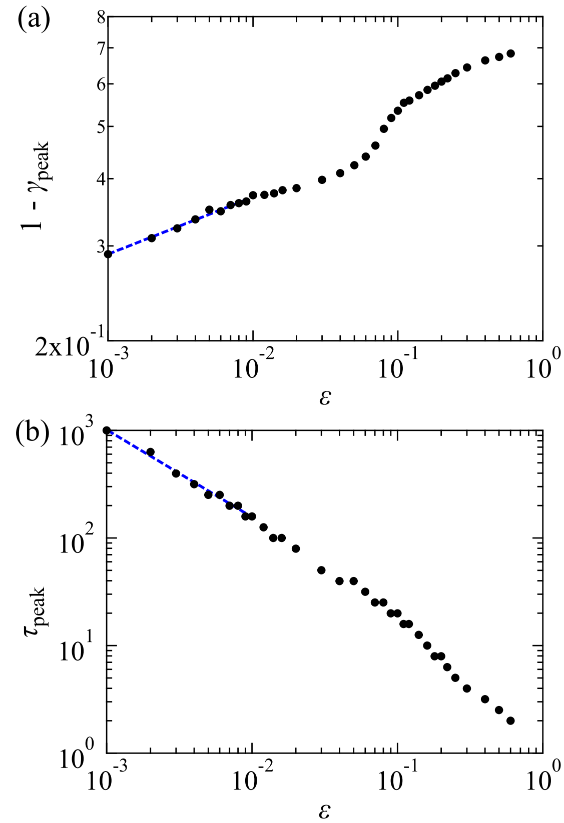

FIG. 7. (a) Value γ_{peak} of the local maximum of $\gamma(\tau)$ and (b) time τ_{peak} when $\gamma(\tau)$ is a local maximum. The blue dashed lines represent the power-law fitting. No local maximum appears in $\gamma(\tau)$ for $\varepsilon \gtrsim 0.7$.

local minima are positive for the control parameters we are investigating.

A notable characteristic of the anomalous parameter in the Nikolaevskii turbulence is that it has a local maximum at the intermediate timescale. Focusing on the peak height γ_{peak}, we find a power law for small ε,

$$\gamma_{peak} - 1 \sim -\varepsilon^{\zeta}, \tag{14}$$

with $\zeta = 0.106 \pm 0.005$, as indicated in Fig. 7(a). Further, the time τ_{peak} at which the anomalous parameter is maximal also holds for a power-law relation

$$\tau_{peak} \sim \varepsilon^{\eta}, \tag{15}$$

with $\eta = -0.812 \pm 0.025$, as indicated in Fig. 7(b). These results suggest that the origin of anomalous diffusion has a scale invariance with small ε.

IV. DISCUSSION

A. Two-scale Brownian motion

The simulation results of $\gamma(\tau)$ show that superdiffusive motion emerges in an intermediate timescale before reaching a normal diffusion timescale. We propose a model, two-scale Brownian motion (2SBM), to explain the superdiffusion as originating from the slow movement of a nonlocal structure.

A tagged particle in the Nikolaevskii turbulence moves randomly due to the disturbed flow. We assume that the

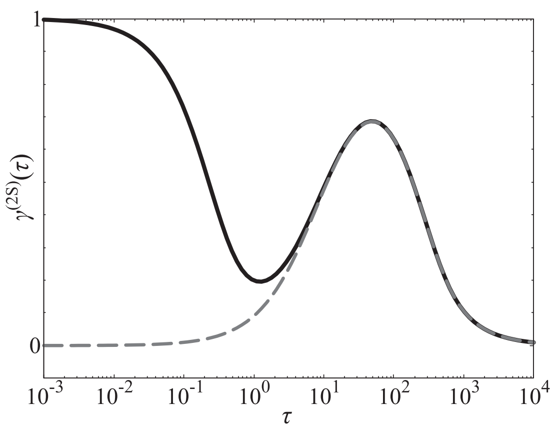

FIG. 8. Anomalous parameter obtained theoretically in 2SBM. The solid line indicates Eq. (23) and the dashed one Eq. (24). The values of the parameters are $\tilde{D} = 20$, $\tau_F = 0.1$, and $\tau_S = 100$.

motion driven by the disturbance is described by the Brownian motion[1] and the momentum relaxation time τ_F is a characteristic time. This timescale stage is called a fast layer. In addition, we assume that the tagged particle is advected by a slow diffusive structure, the dynamics of which is described by the Brownian motion with a slower timescale τ_S. This stage is called a slow layer. Since the dynamics of the structure is ballistic when $\tau \ll \tau_S$, the inertial force due to the advection can be neglected. The tagged-particle dynamics is therefore governed by the stochastic evolution equations

$$\tau_F \frac{d\boldsymbol{V}_F(t)}{dt} = -\boldsymbol{V}_F(t) + \boldsymbol{R}_F(t), \tag{16}$$

$$\tau_S \frac{d\boldsymbol{V}_S(t)}{dt} = -\boldsymbol{V}_S(t) + \boldsymbol{R}_S(t), \tag{17}$$

where the velocity of the tagged particle is $\boldsymbol{V}(t) = \boldsymbol{V}_F(t) + \boldsymbol{V}_S(t)$ and $\boldsymbol{R}_F(t)$ and $\boldsymbol{R}_S(t)$ denote the velocity fluctuations for each layer. It is simply assumed that the fluctuation is white, i.e., $\langle \boldsymbol{R}_F(t)\rangle = \langle \boldsymbol{R}_S(t)\rangle = \mathbf{0}$, $\langle \boldsymbol{R}_F(t+\tau)\boldsymbol{R}_F(t)\rangle = 2D_F\delta(\tau)\mathbf{1}$, and $\langle \boldsymbol{R}_S(t+\tau)\boldsymbol{R}_S(t)\rangle = 2D_S\delta(\tau)\mathbf{1}$, and the different-layer fluctuations are assumed to be independent, where $\mathbf{1}$ denotes the unit matrix and D_F and D_S are the diffusion coefficients for each layer.

The mean-square displacement for 2SBM is represented as

$$M_2^{(2S)}(\tau) = \langle |\boldsymbol{X}_F(\tau) + \boldsymbol{X}_S(\tau)|^2\rangle, \tag{18}$$

where

$$\boldsymbol{X}_*(\tau) = \int_0^\tau \boldsymbol{V}_*(t)dt \quad (* = \text{F or S}) \tag{19}$$

and the initial position is set as the origin. Because the different-layer motions are independent, $M_2^{(2S)}(\tau)$ reduces to

$$M_2^{(2S)}(\tau) = \langle |\boldsymbol{X}_F(\tau)|^2\rangle + \langle |\boldsymbol{X}_S(\tau)|^2\rangle. \tag{20}$$

The evolution equations (16) and (17) lead us to

$$\langle |\boldsymbol{X}_*(\tau)|^2\rangle = 2dD_*\left[\tau - \tau_* + \tau_* \exp\left(-\frac{\tau}{\tau_*}\right)\right], \tag{21}$$

where d denotes the space dimensionality. This equation indicates that the long-time diffusion coefficient of 2SBM is the summation of the diffusion coefficients for each layer. Thus, we obtain

$$M_2^{(2S)}(\tau) = 2dD_F\tau_F\left[(1+\tilde{D})\frac{\tau}{\tau_F} + \exp\left(-\frac{\tau}{\tau_F}\right) - 1 + \tilde{D}\frac{\tau_S}{\tau_F}\exp\left(-\frac{\tau}{\tau_S}\right) - \tilde{D}\frac{\tau_S}{\tau_F}\right], \tag{22}$$

where $\tilde{D} := D_S/D_F$ denotes the ratio of the diffusion coefficients.

Through the time-dependent diffusion coefficient (11), the anomalous parameter for 2SBM can be calculated as

$$\gamma^{(2S)}(\tau) = \frac{\left[(1+\tilde{D}) - \exp\left(-\frac{\tau}{\tau_F}\right) - \tilde{D}\exp\left(-\frac{\tau}{\tau_S}\right)\right]\frac{\tau}{\tau_S}}{(1+\tilde{D})\frac{\tau}{\tau_S} + \frac{\tau_F}{\tau_S}\exp\left(-\frac{\tau}{\tau_F}\right) - \frac{\tau_F}{\tau_S} + \tilde{D}\exp\left(-\frac{\tau}{\tau_S}\right) - \tilde{D}} - 1. \tag{23}$$

This representation has a local minimum and maximum under appropriate parameters and describes the simulation results of $\gamma(\tau)$ in a qualitative manner (Fig. 8). Therefore, from the viewpoint of 2SBM, the appearance of the peak of $\gamma(\tau)$ indicates the existence of hierarchical layers of the diffusive process.

As shown in Fig. 6 for higher ε, i.e., the Kuramoto-Sivashinsky-type turbulence, a gentle peak appears in $\gamma(\tau)$ at a long timescale $\simeq 10^4$. Two-scale Brownian motion has not elucidated this behavior yet.

B. Approximation focusing the local maximum

We next consider an approximated form of Eq. (23) to analyze the peak values of the anomalous parameter. In the timescale $\tau \gg \tau_F$, the mean-square displacement of the fast layer is represented by normal diffusion: $\langle |\boldsymbol{X}_F(\tau)|^2\rangle \simeq 2dD_F\tau$. The anomalous parameter for $\tau \gg \tau_F$ is approximated as

$$\gamma^{(2S)}(\hat{\tau}) \simeq \frac{1 - e^{-\hat{\tau}} - \hat{\tau}e^{-\hat{\tau}}}{(1+\tilde{D})\hat{\tau} - \tilde{D}(1 - e^{-\hat{\tau}})}\tilde{D}, \tag{24}$$

where $\hat{\tau} = \tau/\tau_S$ denotes a normalized time. As shown in Fig. 8, Eq. (24) well approximates Eq. (23) around the local maximum. Equation (24) indicates that both the maximal value $\gamma_{\text{peak}}^{(2S)}$ and the normalized time $\hat{\tau}_{\text{peak}}^{(2S)}$ when $\gamma^{(2S)}(\hat{\tau})$ is maximal depend only on $\tilde{D}$. Further, with the increase of $\tilde{D}$, $\hat{\tau}_{\text{peak}}^{(2S)}$ monotonically decreases and $\gamma_{\text{peak}}^{(2S)}$ monotonically

[1]The term "Brownian motion" is used in a broad sense, that is, the concept of Brownian motion is applied to phenomena that can be separated into a microscopic scale (originally molecular motion) and a macroscopic scale (originally the motion of colloidal particles).

TABLE I. Values of the power-law index for the Nikolaevskii turbulence.

T	Temperature	α_l	1.50±0.00
D_{LT}	Long-time diffusion coefficient	β_l	0.597±0.011
γ_{peak}	Peak value of the anomalous parameter	ζ	0.106±0.005
τ_{peak}	Peak time of the anomalous parameter	η	−0.812±0.025
τ_S	Characteristic time of the slow layer	$\mu_S = -\zeta + \eta$	−0.918±0.030
D_S	Diffusion coefficient of the slow layer	$\nu_S = -\zeta + \eta + \alpha_l$	0.58±0.03
τ_F	Characteristic time of the fast layer	$\mu_F = \zeta + \eta$	−0.706±0.030
D_F	Diffusion coefficient of the fast layer	$\nu_F = \zeta + \eta + \alpha_l$	0.79±0.04

approaches 1. These facts support the peak analysis of $\gamma(\tau)$ being useful to extract the diffusive properties of the hierarchical layers.

For large $\hat{D}$, $\hat{\tau}_{peak}^{(2S)}$ is analytically derived from Eq. (24) as the power law

$$\hat{\tau}_{peak}^{(2S)} \simeq \sqrt{6}\tilde{D}^{-1/2}, \tag{25}$$

and then

$$\gamma_{peak}^{(2S)} \simeq 1 - \frac{2\sqrt{6}}{3}\tilde{D}^{-1/2}. \tag{26}$$

These indicate that $\tau_{peak}/\tau_S \sim 1 - \gamma_{peak}$.

Two-scale Brownian motion does not perfectly describe the simulation results; for example, although the peak of $\gamma(\tau)$ has a shoulder as shown in Fig. 6, 2SBM cannot describe it. Although a more multilayered model might improve the quantitative description, it is unclear whether the more precise description helps in understanding the Nikolaevskii turbulence. One should recall that 2SBM is based on several assumptions such as a Markov property on each layer, the scale separation $\tau_F \ll \tau_S$, and the Einstein relation. In this paper, we do not take account of multilayering models and instead focus on 2SBM to reveal the hierarchical structure in Nikolaevskii turbulence.

C. 2SBM analysis for Nikolaevskii turbulence

The preceding sections suggest that the local maximum of $\gamma(\tau)$ contains essential information. We analyze the simulation results of the Nikolaevskii turbulence from a 2SBM viewpoint. Assuming the power-law relation between the control parameter ε and the ratio $\tilde{D}$ of the different-layer diffusion coefficients, we obtain

$$\tilde{D} \sim \varepsilon^{-2\zeta}, \tag{27}$$

$$\tau_{peak}/\tau_S \sim \varepsilon^{\zeta} \tag{28}$$

from Eqs. (14), (15), (25), and (26). As the diffusion coefficients for each layer are zero at $\varepsilon = 0$, the negative value of the power in Eq. (27) means that the slow-layer diffusion is dominant at sufficiently low ε. Figure 7(b) allows us to evaluate the slow relaxation time as

$$\tau_S \sim \varepsilon^{\mu_S}, \tag{29}$$

with $\mu_S = -\zeta + \eta = -0.918 \pm 0.030$. Because of the Einstein relation, we obtain the diffusion coefficient of the slow layer as

$$D_S \sim \tau_S T \sim \varepsilon^{\nu_S}, \tag{30}$$

with $\nu_S = \mu_S + \alpha_l = 0.58 \pm 0.03$. The values of the power-law index are summarized in Table I including the fast-layer diffusion characteristics τ_F and D_F. The fact that $\beta_l = \nu_S$ within error also supports the fast-layer diffusion being weaker at a sufficiently low ε region. On the other hand, in a higher ε region, i.e., Kuramoto-Sivashinsky-type turbulence, the diffusion coefficient D_{LT} also satisfies the power law; however, it is not equivalent to D_S because the fast-layer fluctuation is not negligible.

A successful description by 2SBM suggests that a slow diffusive structure exists in the Nikolaevskii turbulence at small ε. Sakaguchi and Tanaka showed numerically the amplitude death domain in the Matthews-Cox equations [21]. Although it is unclear whether such domains exist in the Nikolaevskii turbulence, a region separated by the domains might correspond to the slow structure. Nonlocal structures in weak turbulence have been observed experimentally [13,33–36] and theoretically [37–42]. We consider that the existence of such structures can universally characterize the spatiotemporal chaos, as stated in Ref. [36]. The power-law index calculated in this paper will be useful to study the universal feature of weak turbulence.

The slow diffusive structure can explain the existence of a characteristic length of the Nikolaevskii turbulence [22,24]. The length corresponds to the size of the slow structure, and small systems smaller than the slow structure size show behavior different from that of large systems. The investigation of the system size dependence might lead to an understanding of the ε dependence of the slow structure size.

V. SUMMARY

We have studied theoretically the one-dimensional Nikolaevskii turbulence, which is a mathematical model of soft-mode turbulence observed experimentally in nematic electroconvective systems. To understand the properties from the viewpoint of the Lagrangian description, we have simulated numerically the tagged-particle dynamics in the Nikolaevskii turbulence, where the velocity field has been obtained by assuming the convective structure. The tagged particle diffuses due to the turbulent flow, and the anomalous diffusion has been characterized by the mean-square displacement (Fig. 3) and the anomalous parameter (Fig. 6). The anomalous parameter has a local maximum at the intermediate timescale. Further, we have found that slow diffusion is characterized by a power law for the small ε, suggesting that the diffusive property of the structure remains scale invariant. We have proposed a simplified model, referred to as 2SBM, to understand the specific feature. A particle in 2SBM is assumed to move by two mechanisms: fast turbulent fluctuation and advection by a slow diffusive structure. The successful description of the local maximum by 2SBM suggests the existence of a hierarchy in the Nikolaevskii turbulence. In addition, 2SBM has been verified quantitatively by comparing the indices of the diffusion coefficients [Eqs. (12) and (30)]. Since such nonlocal structures have been observed in weak turbulence experimentally and theoretically, the power-law characteristics of the slow diffusive structure might help to understand the universality of the weak turbulence and then will lead to an understanding of the transition to disordered states.

Although we have revealed the diffusive property of the structure, it has not been clarified what the slow structure is. We speculate that the slow structure relates to the Nambu-Goldstone mode. To specify how the zero-wave-number mode affects the slow structure, a possibility is to study the damped Nikolaevskii equation [14,43], which contains friction terms that reduce the long-range mode. It would also be interesting to research three-dimensional systems, i.e., to solve the two-dimensional Nikolaevskii equation, in terms of correspondence with experiments. This is left for future study.

ACKNOWLEDGMENT

The authors gratefully acknowledge Professor Hidetsugu Sakaguchi (Kyushu University) for fruitful discussions. This work was supported by KAKEHNI (Grant No. JP17K14593).

[1] G. Falkovich, K. Gawedzki, and M. Vergassola, Rev. Mod. Phys. **73**, 913 (2001).

[2] H. Aref, J. R. Blake, M. Budišić, S. S. S. Cardoso, J. H. E. Cartwright, H. J. H. Clercx, K. El Omari, U. Feudel, R. Golestanian, E. Gouillart *et al.*, Rev. Mod. Phys. **89**, 025007 (2017).

[3] O. Reynolds, Philos. Trans. R. Soc. London **174**, 935 (1883).

[4] H. Y. Shih, T. L. Hsieh, and N. Goldenfeld, Nat. Phys. **12**, 245 (2016).

[5] G. Lemoult, L. Shi, K. Avila, S. V. Jalikop, M. Avila, and B. Hof, Nat. Phys. **12**, 254 (2016).

[6] M. Sano and K. Tamai, Nat. Phys. **12**, 249 (2016).

[7] P. Manneville, *Dissipative Structure and Weak Turbulence* (Academic Press, San Diego, 1990).

[8] M. Dennin, G. Ahlers, and D. S. Cannell, Science **272**, 388 (1996).

[9] Y. Hidaka and N. Oikawa, Forma **29**, 29 (2014).

[10] V. N. Nikolaevskii, in *Recent Advances in Engineering Sciences*, edited by S. L. Koh and C. G. Speciale (Springer, Berlin, 1989), pp. 210–221.

[11] M. I. Tribelsky and K. Tsuboi, Phys. Rev. Lett. **76**, 1631 (1996).

[12] P. C. Matthews and S. M. Cox, Phys. Rev. E **62**, R1473 (2000).

[13] Y. Hidaka, K. Tamura, and S. Kai, Prog. Theor. Phys. Suppl. **161**, 1 (2006).

[14] S. M. Cox and P. C. Matthews, Phys. Rev. E **76**, 056202 (2007).

[15] H. Fujisaka and T. Yamada, Prog. Theor. Phys. **106**, 315 (2001).

[16] D. Tanaka, Phys. Rev. E **70**, 015202(R) (2004).

[17] D. Tanaka, Prog. Theor. Phys. Suppl. **161**, 119 (2006).

[18] S. Kai, K.-I. Hayashi, and Y. Hidaka, J. Phys. Chem. **100**, 19007 (1996).

[19] Y. Hidaka, J.-H. Huh, K.-I. Hayashi, S. Kai, and M. I. Tribelsky, Phys. Rev. E **56**, R6256 (1997).

[20] Y. Hidaka, J.-H. Huh, K.-I. Hayashi, M. I. Tribelsky, and S. Kai, J. Phys. Soc. Jpn. **66**, 3329 (1997).

[21] H. Sakaguchi and D. Tanaka, Phys. Rev. E **76**, 025201(R) (2007).

[22] D. Tanaka and M. Okamura, J. Phys. Soc. Jpn. **79**, 124004 (2010).

[23] A. S. Monin and A. M. Yaglom, *Statistical Fluid Mechanics: Mechanics of Turbulence* (MIT Press, Cambridge, 1971).

[24] T. Narumi and Y. Hidaka (unpublished).

[25] S. M. Cox and P. C. Matthews, J. Comput. Phys. **176**, 430 (2002).

[26] M. Cross and H. Greenside, *Pattern Formation and Dynamics in Nonequilibrium Systems* (Cambridge University Press, Cambridge, 2009).

[27] H. Sakaguchi, Int. J. Mod. Phys. B **17**, 4338 (2003).

[28] M. Suzuki, H. Sueto, Y. Hosokawa, N. Muramoto, T. Narumi, Y. Hidaka, and S. Kai, Phys. Rev. E **88**, 042147 (2013).

[29] D. Tanaka, Phys. Rev. E **71**, 025203(R) (2005).

[30] F. Nugroho, H. Hamadi, Andi, D. T. Ridlo, Y. Yusuf, P. Nurwantoro, A. Setiawan, T. Narumi, and Y. Hidaka (unpublished).

[31] Y. Hidaka, Y. Hosokawa, N. Oikawa, K. Tamura, R. Anugraha, and S. Kai, Physica D **239**, 735 (2010).

[32] J. Klafter, M. F. Shlesinger, and G. Zumofen, Phys. Today **49**(2), 33 (1996).

[33] N. Oikawa, Y. Hidaka, and S. Kai, Prog. Theor. Phys. Suppl. **161**, 320 (2006).

[34] K. A. Takeuchi, M. Kuroda, H. Chaté, and M. Sano, Phys. Rev. Lett. **99**, 234503 (2007).

[35] N. Oikawa, Y. Hidaka, and S. Kai, Phys. Rev. E **77**, 035205(R) (2008).

[36] T. Narumi, Y. Mikami, T. Nagaya, H. Okabe, K. Hara, and Y. Hidaka, Phys. Rev. E **94**, 042701 (2016).

[37] K. Kaneko, Prog. Theor. Phys. **74**, 1033 (1985).

[38] Y. Pomeau, Physica D **23**, 3 (1986).

[39] H. Chaté and P. Manneville, Phys. Rev. Lett. **58**, 112 (1987).

[40] S. Ciliberto and P. Bigazzi, Phys. Rev. Lett. **60**, 286 (1988).

[41] F. Daviaud, M. Bonetti, and M. Dubois, Phys. Rev. A **42**, 3388 (1990).

[42] M. M. Degen, I. Mutabazi, and C. D. Andereck, Phys. Rev. E **53**, 3495 (1996).

[43] E. Simbawa, P. C. Matthews, and S. M. Cox, Phys. Rev. E **81**, 036220 (2010).